Electrochimica Acta 134 (2014) 242–248

Contents lists available at ScienceDirect

Electrochimica Acta

journal homepage: www.elsevier.com/locate/electacta

Influence of substrate morphology on the growth and properties of TiO_2 nanotubes in HBF_4-based electrolyte

Junheng Xing, Hui Li, Zhengbin Xia*, Jiangqiong Chen, Yanhong Zhang, Li Zhong

School of Chemistry and Chemical Engineering, South China University of Technology, Guangzhou, Guangdong 510641, China

ARTICLE INFO

Article history:
Received 5 March 2014
Received in revised form 2 April 2014
Accepted 21 April 2014
Available online 28 April 2014

Keywords:
Titanium
Nanotube
Anodization
Self-assembly
HBF_4

ABSTRACT

The present work demonstrates how the growth and photoelectrochemical (PEC) properties of anodic TiO_2 nanotubes (NTs) are influenced by Ti substrates in the new HBF_4 containing electrolyte. Three different Ti substrates, the rough abraded Ti foil, the smooth electropolished Ti and the two-step Ti plate (i.e. the Ti substrate with ordered dimples left by removing the TiO_2 NTs formed in the first-step anodization), are employed for the preparation of TiO_2 NTs. It is revealed that the Ti substrate morphology can largely influence the formation of TiO_2 NTs, particularly in the initial tube generation stage. The two-step Ti substrate has ordered hexagonally distributed dimples which play the role of template for the formation of new TiO_2 NTs. As a result, the TiO_2 NTs grown via a two-step anodization approach have highly ordered structure and extremely smooth sidewalls, hence possess the best PEC performance among the three kinds of substrates.

1. Introduction

Regular self-organized TiO_2 nanotubes (NTs) prepared by electrochemical anodization methods have found their applications in many areas, such as solar cells, photocatalysis, sensors and batteries, due to the unique 1-dimensional nanostructure [1–4]. In general, the TiO_2 NTs are usually fabricated in fluoride ions (F^-) containing organic or aqueous electrolyte, and their structure and properties are mainly determined by the applied potentials, F^- concentration, H_2O content and anodizing time [3,5,6]. Nevertheless, the TiO_2 NTs formed in F^- containing electrolyte have their limitations, for example, the easy formation of ripples along the sidewalls, because of the highly aggressive of F^- [7–9]. Recently, efforts have been dedicated to develop new electrolyte systems for the fabrication of TiO_2 NTs. One newly development is using a mild, BF_4^- containing electrolyte system. Schmuki et al. showed that TiO_2 NTs with the length of about 650 nm could be successfully prepared in ionic liquid (IL, BMIM-BF_4) containing small amount of water [10]. Subsequently, this technique was developed by Misra et al. and Wender et al. in organic electrolyte containing IL and water [11,12]. Although the produced NTs in those IL-based electrolytes have disordered structure and very limited length, their studies indicate that TiO_2 NTs can be formed in electrolyte containing complex fluoride ions, such as BF_4^-, which provides us an alternative way for the preparation of TiO_2 NTs [10–15].

The surface morphology of Ti substrate can greatly influence the growth and properties anodic TiO_2 NTs [16,17]. In general, the as-purchased Ti samples and the conventional mechanically abraded Ti substrates are usually very rough, making them not good candidates for preparation of regular TiO_2 NTs [18]. After long time anodization of those substrates in F^- containing electrolyte (to grow TiO_2 NTs with enough length), chemical attack of the tube mouth easily takes place, which leads to the "nanograss" appearance on the top of the NTs [19]. To avoid this disadvantage, Kim et al. used smooth mechanically polished Ti samples for the fabrication of TiO_2 NTs, and found that a top porous layer was formed, which can effectively protect the underneath NTs from corrosion by the solution anions [19]. Similarly, as reported by Smith et al., the hierarchical TiO_2 NTs with a top nanoporous layer and regular underneath NTs were produced by using chemically polished Ti substrate, which showed enhanced photoelectrochemical (PEC) performance [20]. Electrochemical polishing is another often cited method for the surface optimization of Ti foils. As shown by Lee et al., the electropolished Ti specimens had relatively smooth surface, which was beneficial to the preparation of highly ordered TiO_2 NTs [21]. In brief, the Ti substrates are usually pretreated by various polishing methods before anodization to obtain TiO_2 NTs with desirable structure. Nevertheless, as argued by Zhang et al., Ti substrates with extremely flat surface were

* Corresponding author. Tel.: +86 20 8711 2047; fax: +86 20 8711 2093.
E-mail address: cezhbxia@scut.edu.cn (Z. Xia).

http://dx.doi.org/10.1016/j.electacta.2014.04.120
0013-4686/

not always necessary to the growth of ordered TiO_2 NTs, in other words, the formed porous top layer with randomly distributed nanopores was not beneficial to the underneath TiO_2 NTs growth [22].

Recently, a two-step anodization method, firstly reported by Masuda et al. for aluminum [23,24], has been widely adopted for the fabrication of highly ordered TiO_2 NTs, mainly in F^- contained organic electrolyte [21,22,25,26]. By removing the relatively disordered NTs grown in the first-step anodization, very ordered hexagonal imprint patterns are left on Ti substrates (i.e. the two-step Ti substrate), which further play the role of template for the generation of new NTs, and then greatly improve the uniformity and orderliness of the TiO_2 NTs during the second-step anodization [22]. The obtained two-step TiO_2 NTs usually have unique hierarchical upper-porous and lower-tubular structure, and have been defined as the new generation of TiO_2 NTs [22,25,27–29].

As presented above, the structure and properties of TiO_2 NTs are largely determined by the surface morphology of Ti substrate. Nevertheless, for the growth mechanisms of TiO_2 NTs on different Ti substrates (particularly at the beginning of anodization), it is rarely addressed. In this paper, regular TiO_2 NTs with smooth sidewalls are produced in the unique HBF_4-based electrolyte using three different Ti substrates, i.e. the relatively rough mechanically abraded Ti specimen, the smooth electropolished Ti sample and the two-step Ti substrate. The formation of TiO_2 NTs in BF_4^- containing electrolyte is investigated and the influence of substrates on the growth and properties of TiO_2 NTs is discussed in detail.

2. Experimental Section

2.1. Preparation of TiO_2 NTs

In the present work, highly pure Ti sheets (> 99.99%, 1 mm thick) with the size of 13 × 10 mm were employed for the preparation of TiO_2 NTs. Before anodization, the Ti samples were pretreated by three different methods. The first substrate was mechanically abraded with 600, 1000 and finally with 1500 emery papers and then chemically etched in a solution of 1% HF and 3% HNO_3 for about 4 s. For the second Ti substrate, the as-abraded Ti (i.e. the first Ti substrate) was electrochemically polished with a mixed solution of ethanol, butanol and perchloric acid (with the volume of 9:6:1) at 20 V for 5 min at 0 °C (the method was originally from Shin and Lee [21]). In the case of the third Ti substrate, the as-abraded Ti was first anodically treated in ethylene glycol (EG) electrolyte containing 0.5 wt% HBF_4 and 5 vol% H_2O at 80 V for 30 min, and then the formed TiO_2 NTs were peeled off by ultrasonication in deionized water. After pretreatments, all the Ti substrates were ultrasonically cleaned with ethanol for 20 min and later with deionized water for 20 min. Anodizing of Ti was carried out in a two-electrode cell at room temperature, maintained by a DC power, a Pt plate was used as the counter electrode. The TiO_2 NTs were fabricated on different Ti substrates in HBF_4-based electrolyte (EG + 0.5 wt% HBF_4 + 5 vol% H_2O) at 80 V for 30 min. After preparation, all the anodic samples were annealed at 450 °C for 2 h.

2.2. Characterization of TiO_2 NTs

The surface roughness (root mean square roughness, R_{ms}) of different Ti substrates was measured by atomic force microscope (AFM, BENYUAN CSPM 4000, China). The surface morphologies of different Ti substrates and the produced anodic TiO_2 NTs were detected by a Scanning electron microscope (SEM, NOVA NANOSEM 430, Holland) which was performed with the electron beam of 15 kV. The crystallization of the obtained TiO_2 NTs was determined by a Raman spectrometer (HORIBA Jobin Yvon LabRAM Aramis, France) and an X-ray diffractometer (XRD, Bruker D8 ADVANCE, Germany). The Raman spectra were recorded with the excitation wavelength of 532 nm and the line incidence power of 10.4 mW. The XRD measurements were operated by using a Cu Kα (1486.6 eV) radiation source at 30 kV and 30 mA. The chemical compositions of

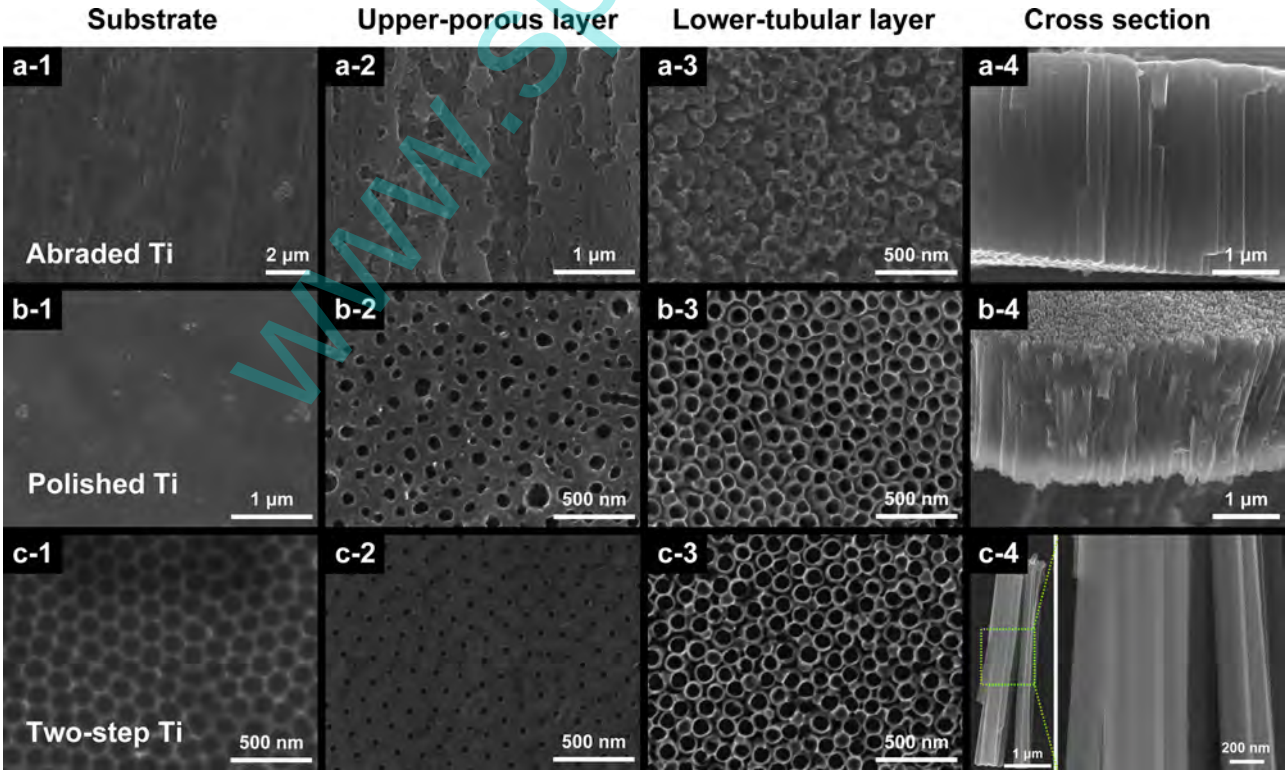

Fig. 1. SEM images of different Ti substrates and TiO_2 NTs grown on the corresponding substrates.

the TiO_2 NTs were tested by an X-ray photoelectron spectrometry (XPS, Kratos Axis Ultra DLD, UK) which was carried out with an Al Kα (1486.6 eV) radiation source at 15 kV and 150 W. The peak positions of the XPS spectra were corrected by setting the C 1s peak at 284. 6 eV, and during the fitting of the obtained peaks, the Shirley background was employed.

2.3. PEC measurement

The PEC properties of the prepared TiO_2 NTs on different Ti substrates were tested with a conventional three-electrode cell which was equipped with a platinum plate as the counter electrode and Ag/AgCl as the reference electrode. The experiments were carried out in 1 M KOH solution and controlled by an electrochemical workstation. The potential were reported against the reversible hydrogen electrode (RHE) via the following equation:

$$E_{RHE} = E_{Ag/AgCl} + 0.059pH + E^{\circ}_{Ag/AgCl} \quad (1)$$

where $E^{o}_{Ag/AgCl}$ equal to 0.198 V at 25 °C. The produced TiO_2 NTs were illuminated under stimulated solar light (AM 1.5, 100 mW cm^{-2}) from a PLS-SXE300UV Xe lamp (Changtuo, China). For the PEC measurements, more than five samples were prepared and tested for every Ti substrate, and the results exhibited good reproducibility (with the error less than 20%).

3. Results and Discussion

3.1. Surface morphology

Fig. 1 presents the SEM images of different Ti samples and the obtained TiO_2 NTs on the corresponding substrates. The as-abraded Ti substrate is very rough (with the R_{ms} of about 37.0 nm, as can be found in our previous work [18]) and contains numerous local defects (Fig. 1(a-1)). After electrochemical polishing treatment for the Ti sample, relatively smooth surface (with the R_{ms} of approximately 11.6 nm, as measured by AFM) can be obtained (Fig. 1(b-1)). For the two-step Ti substrate, after removing the TiO_2 NTs formed in the first-step anodization, very regular hexagonally distributed dimples are left on the Ti surface (Fig. 1(c-1)). As shown in Fig. 1, in difference to the traditional TiO_2 NTs formed in F^- contained electrolyte, the TiO_2 NTs grown in BF_4^- containing solution have unique hierarchical upper-porous and lower-tubular structure in spite of the used Ti substrates, and as will be discussed later, this is probably due to the less aggressive of BF_4^- [11].

First, for the TiO_2 NTs anodically grown on the as-abraded Ti (denoted as A-TiO_2 NTs), the upper layer is very rough, with lots of small nanopores mainly distributed along the scratch line (Fig. 1(a-2)). Underneath the porous top layer, self-organized TiO_2 NTs can be seen, which have very small inner tube diameter and weak ordered structure (Fig. 1(a-3)). From the cross-sectional views, smooth nanotube arrays with the length of about 3.25 μm are shown for the A-TiO_2 NTs (Fig. 1(a-4)). Second, the produced TiO_2 NTs on flat elelctropolished Ti substrate (marked as E-TiO_2 NTs) have relatively smooth upper-porous layer, the nanopores are randomly distributed with the size much larger than that of the A-TiO_2 NTs (Fig. 1(b-2)). As displayed in Fig. 1(b-3), relatively ordered NTs with large inner diameter can be seen for the lower-tubular layer of the E-TiO_2 NTs, which is also different from that of the A-TiO_2 NTs. However, poor arrangement can be seen for the E-TiO_2 NTs from the cross-sectional views, in which the obtained NTs have rough sidewalls and are about 2.24 μm in length (Fig. 1(b-4)).

Last, in the case of the two-step TiO_2 NTs (labeled as T-TiO_2 NTs), ordered hexagonally distributed nanopores, with the uniform size of about 26.7 nm, can be found for the upper-porous layer (Fig. 1(c-2)), which is in good agreement with the regular imprints left by the first-step NTs. By partly removing the thin porous top layer with ultrasonication method, uniform and regular self-organized TiO_2 NTs can be seen for the lower-tubular layer (Fig. 1(c-3)). Moreover, the T-TiO_2 NTs are extremely smooth (which is more clear in the high magnification images of the cross-section of the T-TiO_2 NTs), with the tube length of approximately 4.65 μm (Fig. 1(c-4)). To the best of our knowledge, such smooth tube walls have been rarely reported for the TiO_2 NTs produced in traditional F^- containing electrolyte, and as mentioned by some authors, the smooth sidewalls are beneficial to the electron transport cross the NTs, and then effectively enhance the application performances of the TiO_2 NTs [5].

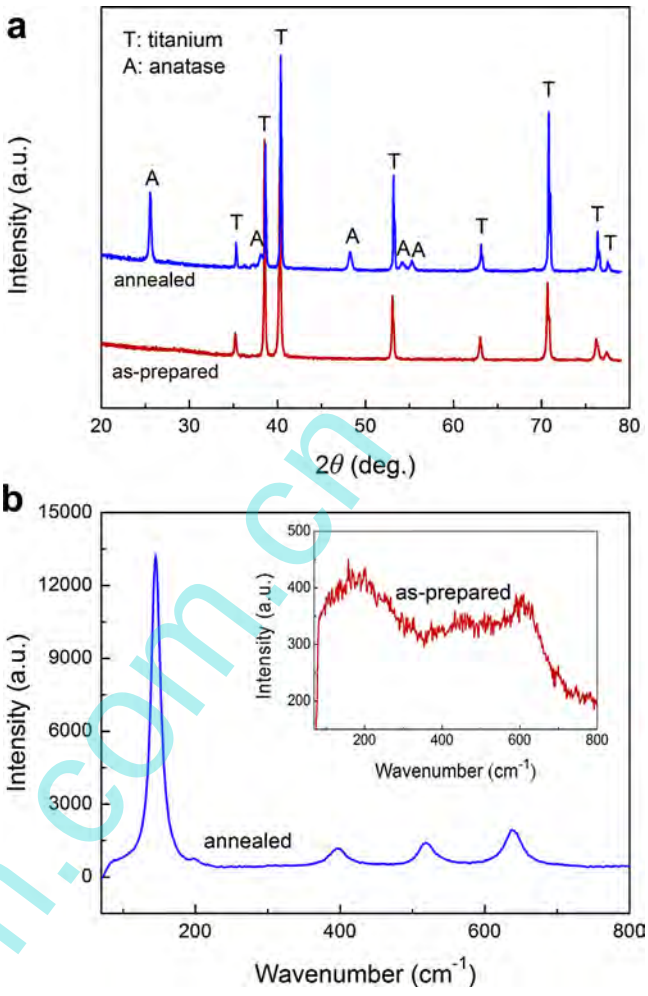

Fig. 2. (a) XRD patterns of and (b) Raman spectra of as-formed and annealed TiO_2 NTs at 80 V for 30 min by using two-step anodization method.

3.2. Crystallization and chemical composition

In different from the surface morphology, the crystalline behavior and chemical compositions of the TiO_2 NTs formed on different Ti substrates do not show some major differences (at least from our present measurements), therefore, we here only present the experiment results of the T-TiO_2 NTs. As shown from the XRD patterns, the as-prepared T-TiO_2 NTs are amorphous, which is the same as the common TiO_2 NTs produced by F^- containing electrolyte [27,29]. While after annealing at 450 °C for 2 h, the structure of the T-TiO_2 NTs converts to anatase (Fig. 2(a)). Similar findings can be also proved by the Raman results, in which no clear peaks can be detected for the unannealed T-TiO_2 NTs, while four Raman peaks at 144 cm^{-1}, 399 cm^{-1}, 516 cm^{-1} and 639 cm^{-1}, attributed to anatase [18], can be clearly found for the annealed NTs (Fig. 2(b)).

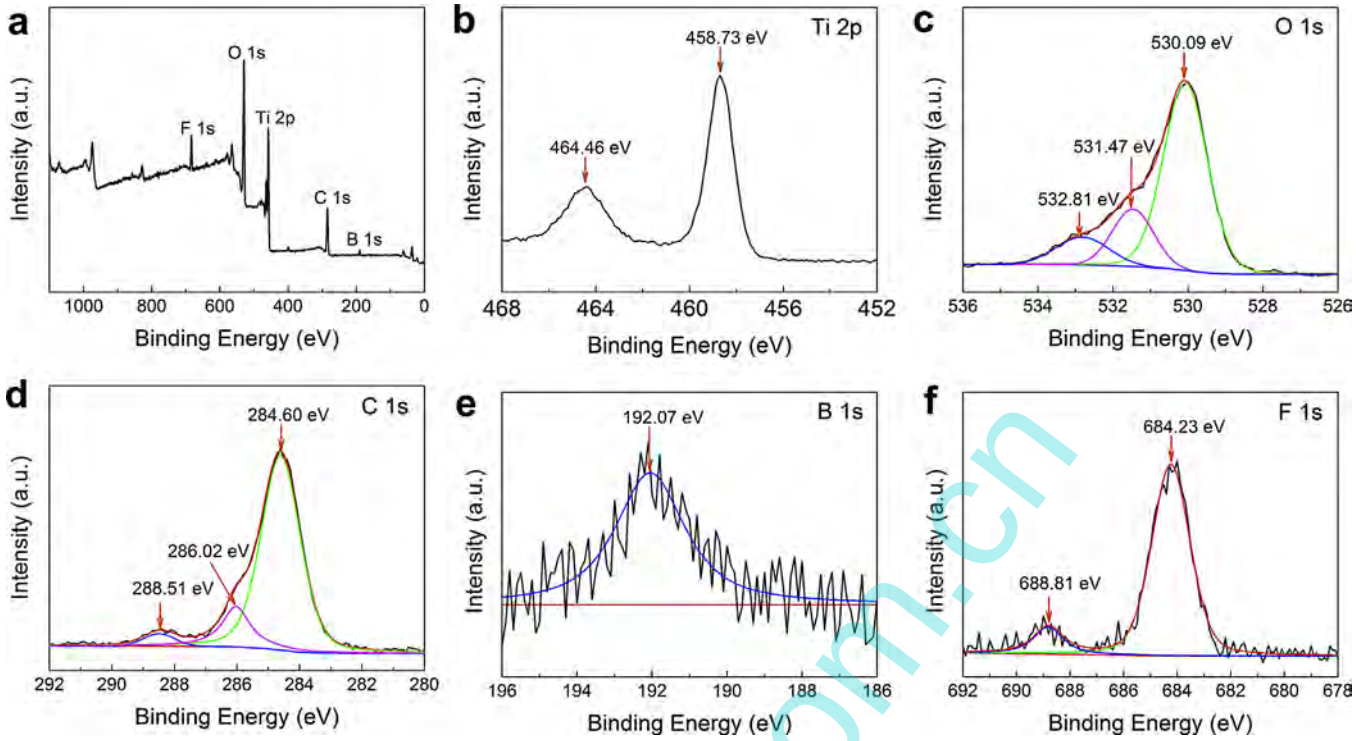

Fig. 3. (a) Survey and (b) Ti 2p, (c) O 1s, (d) C 1s, (e) B 1s and (f) F 1s XPS spectra of anodic TiO_2 NTs prepared at 80 V for 30 min via a two-step anodization approach.

Fig. 3 shows the chemical compositions of the T-TiO_2 NTs. From Fig. 3(a), it can be found that the TiO_2 NTs formed in HBF_4-based electrolyte are mainly composed of Ti 2p, O 1s, C 1s and F 1s elements, and also include a small amount of B 1s. For the Ti 2p XPS spectrum, two peaks at about 458.73 eV and 464.46 eV, both attributed to Ti^{4+}, can be seen (Fig. 3(b)). As for the O 1s spectrum, the three peaks at 530.09 eV, 531.47 eV and 532.81 eV are attributed to Ti-O bond, Ti-OH bond, and absorbed water or carbon impurity (C–OH/C–O–C bonds), respectively (Fig. 3(c)) [30,31]. This reveals that the surface of the formed TiO_2 NTs contains a few Ti hydroxides. The C 1s spectrum can be resolved into three peaks, the largest peak at 284.6 eV is corresponding to C–C/C–H bonds, the second peak at 286.02 eV belongs to C–OH and C–O–C groups, which is in good agreement with the O 1s peak at 532.81 eV, the last peak at 288.51 eV is attributed to–OC = O bond (Fig. 3(d)) [26]. As revealed by Schmuki et al., the–OC = O bond can effectively prevent film breakdown during anodizing process, and then be beneficial to the formation of smooth and ordered TiO_2 NTs [32]. For the B 1s spectrum, a weak peak emerges at 192.07 eV, which indicates that little B element is doped into the TiO_2 lattice (Fig. 3(e)) [33]. The F 1s spectrum can be fitted with two peaks, the major peak at 684.23 eV is attributed to Ti-F bond, whereas the small peak at 688.81 eV is assigned to the doped F (Fig. 3(f)) [34]. In brief, the XPS results suggest that via a simple anodization process, the non-metal elements of F and B, come from the BF_4^- containing solution, are successfully doped into the TiO_2 lattice, which can therefore improve their application performances (such as PC activities) [33–35].

3.3. PEC performance

Anodic TiO_2 NTs exhibit high PEC activities for their unique 1-dimensional nanostructure, hence have been widely studied in the fields of water splitting, pollutants degradation and solar cells [25,27,32]. It is reported that the PEC performances of TiO_2 NTs are largely determined by their geometrical features, such as tube arrangement, length, pore diameter and wall roughness [27,36], and the hierarchically structured TiO_2 NTs were revealed to show higher PEC activities as compared to the common TiO_2 NTs [25,28,37]. The influence of Ti substrates on the PEC properties of the obtained TiO_2 NTs is displayed in Fig. 4. As shown in Fig. 4(a), among all the three samples, the T-TiO_2 NTs produce the highest photocurrent density of about 1.28 mA cm^{-2} at the potential of 1.23 V vs. RHE (which is related to the potential of water oxidation [27]) under illumination of simulated solar light (AM 1.5, 100 mW cm^{-2}). By contrast, the A-TiO_2 NTs show a photocurrent density of about 0.65 mA cm^{-2}, which is lower than the other two samples. Fig. 4(b) presents the amperometric curves of three different types of TiO_2 NTs at 1.23 V vs. RHE with 10 s on/off cycles. It is shown that the A-TiO_2 NTs have lower photocurrent density as compared to the E-TiO_2 NTs and T-TiO_2 NTs, probably due to their very rough surface (see Fig. 1(a-2)) which may enhance the recombination of photogenerated electrons and holes.

To sum up, the T-TiO_2 NTs own the best PEC performance among the three samples, this is mainly because that the T-TiO_2 NTs have very ordered upper-nanoporous layer and regular and extremely smooth nanotube arrays. By contrast, the obtained A-TiO_2 NTs exhibit very rough top layer and weak ordered structure, hence generate the lowest photocurrent density. As for the E-TiO_2 NTs, although they own relatively smooth upper layer, the underneath NTs have rough sidewalls, therefore, their PEC property is not as well as the T-TiO_2 NTs.

3.4. Influence of Ti substrates on growth and properties of TiO_2 NTs

As stated above, we show the effect of Ti substrates on the surface morphology and PEC performances of the fabricated anodic TiO_2 NTs. Nevertheless, the influence mechanisms of the Ti substrate morphology on the growth and properties of TiO_2 NTs need further discussion. To begin with, we firstly give a short review on the formation of TiO_2 NTs in the conventional F^- containing electrolyte. In the beginning of the anodization, a barrier TiO_2 layer

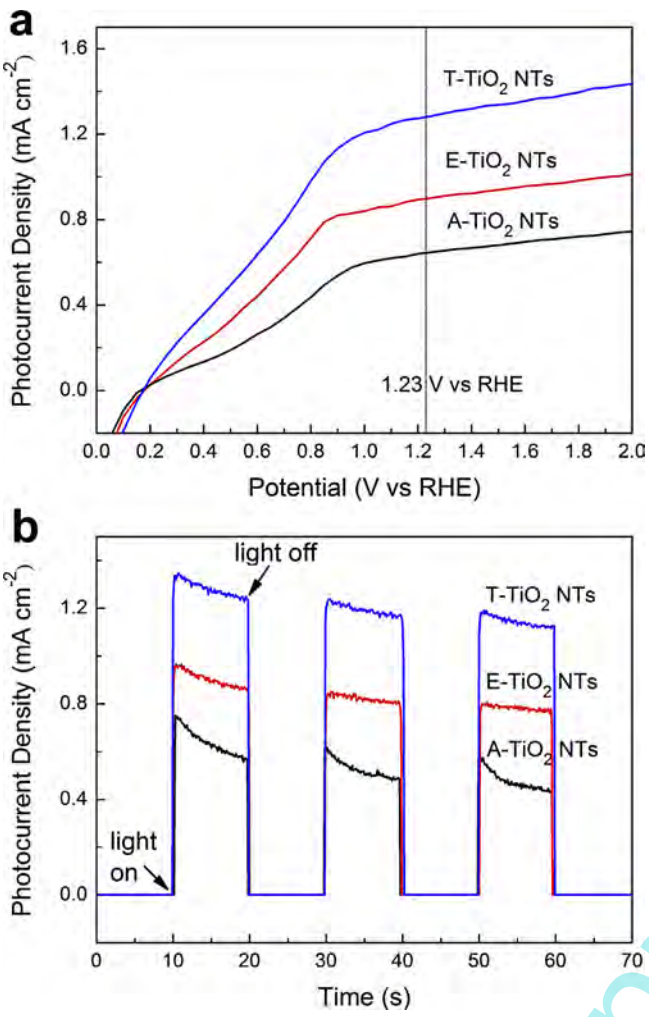

Fig. 4. Photoelectrochemical properties of anodic TiO_2 NTs obtained on different Ti substrates: (a) linear-sweep voltammograms obtained with the potential sweep rate of 5 mV s^{-1}; (b) amperometric curves recorded at an applied voltage of 1.23 V (vs. RHE).

is initially formed, and subsequently, due to the existence of the aggressive F^-, chemical pitting (or say local breakdown) of the barrier layer randomly takes place. Then the pitting sites act as seeds for the growth of the underneath nanopores. Lastly, regular TiO_2 NTs are generated via a self-organization (or say autocatalysis) process, and meanwhile, the initial barrier layer (which is porous layer now) is completely dissolved by the F^- from the solution [38–40].

In our present work, a unique BF_4^- containing electrolyte is used for the fabrication of TiO_2 NTs. The main difference between the two different electrolyte systems is that the complex fluoride ions BF_4^- is less aggressive as compared to F^- [11], and this may lead to two consequences. Firstly, as displayed in Fig. 5, under high electric field, the F^- can be generated from BF_4^- via the reaction: $BF_4^- \rightarrow BF_3 + F^-$ [41],which plays the key role for the growth of TiO_2 NTs in BF_4^- containing electrolyte. At the bottoms of NTs, the highest electric field usually emerges, therefore, sufficient F^- are generated to sustain the growth of TiO_2 NTs [22]. This may mean that the TiO_2 NTs can be grown with high efficiency in BF_4^- electrolyte through this unique mechanism. Moreover, for the reason that the tube inner walls usually have relatively low electric field, therefore few F^- are generated, which means that robust NTs with thick tube walls are more likely formed in BF_4^--based solution. Secondly, the porous top layer, which is easily dissolved in F^- containing solution, is relatively stable in BF_4^- containing electrolyte,

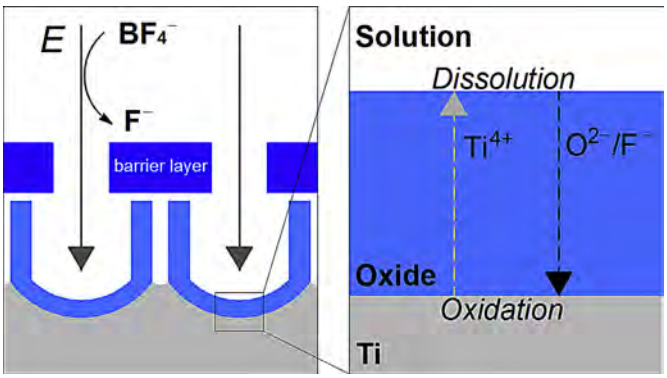

Fig. 5. Schematic illustration of the growth of TiO_2 NTs in BF_4^- containing solution.

hence will not be dissolved away during the anodization process, and our present findings also show that small amounts of titanium hydroxides are deposited onto the top layer (see Fig. 3(c)). This may be the main reason why the TiO_2 NTs grown on different Ti substrates in BF_4^- containing electrolyte all show the hierarchical structure (see Fig. 1). The stable porous upper layer can effectively protect the underneath NTs from corrosion by the anions in the solution [19].

Figure 5 Based on the above theories, the formation mechanisms of TiO_2 NTs on different Ti substrates in HBF_4-based electrolyte are put forward and shown in Fig. 6. The as-abraded Ti exhibits very rough surface which has lots of local defects (see Fig. 1(a-1)). A layer of titanium oxides is firstly generated in the very early stage of the anodization process (Fig. 6(a-1)). The distribution of electric field on the rough oxide film surface is nonuniform, the highest electric field takes place at the defect sites, which further produce lots of F^-. As a result, chemical pitting of TiO_2 barrier layer is prone to occur at the local defect sites (Fig. 6(a-2)). Moreover, our previous findings showed that, under the same condition, the TiO_2 film grown on rougher Ti substrate is much thicker than that formed on smoother Ti surface [42]. For the reason that the thick TiO_2 layer is unfavorable for the ionic migration, the nanoholes of the upper layer, induced by chemical pitting, are relatively small (see Fig. 1(a-2)). Subsequently, small nanopores are generated underneath the anodic oxide layer by direction of the upper pitting holes (Fig. 6(a-3)). As the anodizing time prolonging, a layer of Ti oxides, which exist as $Ti(OH)_xO_y$, are deposited onto the porous top layer as a result of the presence of relatively low electric field. To the last, through an autocatalysis sequence [39], weak ordered TiO_2 NTs with small inner diameter are produced (Fig. 6(a-4)). It is obviously that the thick and rough top layer is not beneficial for the underneath NTs growth.

The electropolished Ti substrate has relatively flat surface, which means that, at the beginning of the anodization, the grown TiO_2 compact layer is very thin and smooth (Fig. 6(b-1)). The electric field is uniformly distributed on the smooth TiO_2 film, and as a result, chemical pitting of the oxide layer randomly takes place (Fig. 6(b-2)). Moreover, the uniform distribution of the electric field may give rise to another consequence, i.e. the neighbouring small pitting holes may aggregate together and lead to large porous structure (see Fig. 1(b-2)). After then, nanopores are generated underneath the porous top layer (Fig. 6(b-3)). The upper oxide layer of the E-TiO_2 NTs is very thin and has relatively large pitting holes, which are both beneficial to the ionic transport. As a result, more F^- are produced, meaning that the TiO_2 NTs will grow in more aggressive condition. This is why the E-TiO_2 NTs have relatively rough tube walls (see Fig. 1(b-4)). As presented in Fig. 6(b-4), regular self-assembly TiO_2 NTs with thin porous upper layer are lastly formed on the electropolished Ti substrate. Meanwhile, a few of Ti

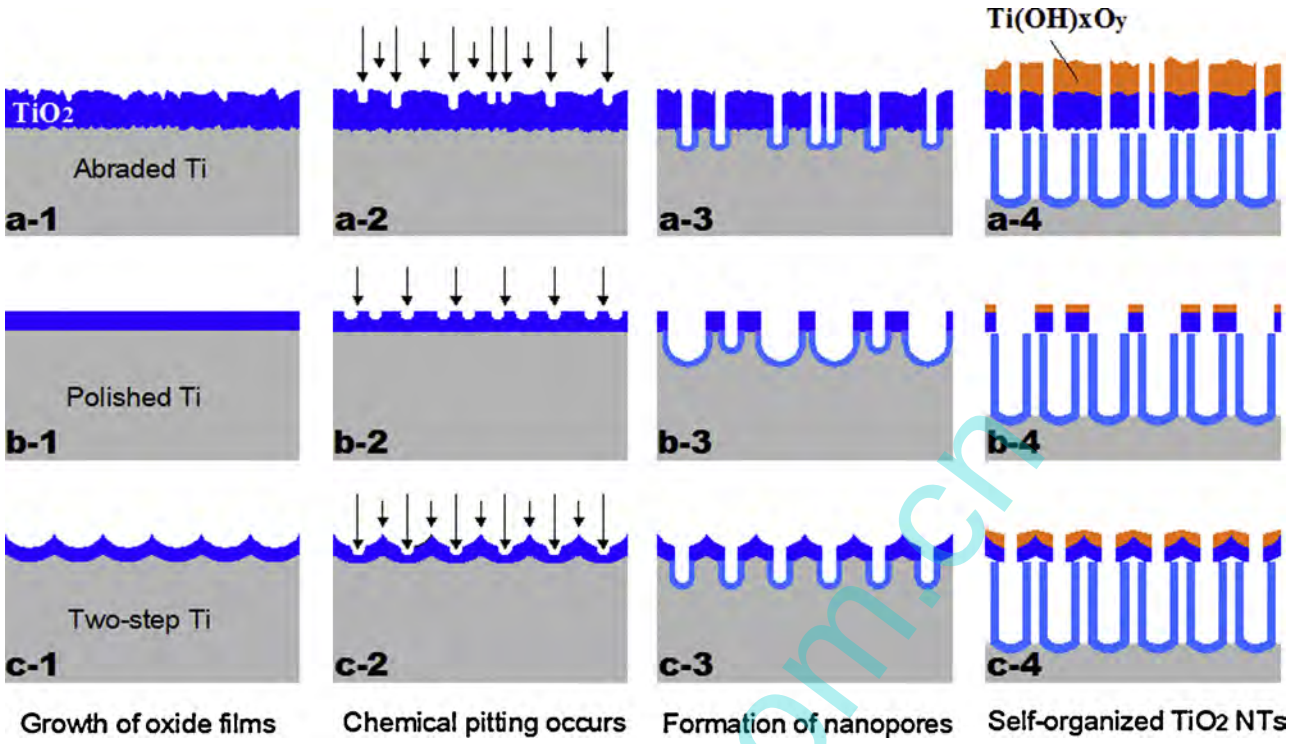

Fig. 6. Schematic representation of the dependence of Ti substrates on the growth of TiO_2 NTs in HBF_4-based electrolyte.

hydroxides are also deposited onto the top layer. This kind of thin porous upper layer with large nanopores can partly enhance the application properties of the TiO_2 NTs (see Fig. 4), while fails to effectively protect the underneath NTs growth. This means that the flat Ti substrates are not necessary for the preparation of highly ordered TiO_2 NTs in BF_4^- containing solution.

After removing the NTs formed in the first-step anodization, hexagonally ordered dimples are left on the two-step Ti substrate (see Fig. 1(c-1)). As shown in Fig. 6(c-1), a barrier layer of TiO_2 is firstly generated in the initial stage of anodization. The electric field distribution is not uniform, at the bottoms of the imprint patterns, the highest electric field usually arises. This means that the chemical pitting is prone to occur at bottoms of the dimples (Fig. 6(c-2)). Subsequently, nanopores are generated underneath the upper layer guided by the uniformly distributed pitting holes (Fig. 6(c-3)). Lastly, through a general self-assembly process, hierarchical TiO_2 NTs with high orderliness and extremely smooth sidewalls are grown on two-step Ti substrate (Fig. 6(c-4)). The stable and ordered upper porous layer of the T-TiO_2 NTs possesses both the benefits of the thick top layer of the A-TiO_2 NTs and the smooth upper layer of the E-TiO_2 NTs, i.e. they can effectively protect the underneath NTs growth (which gives rise to ordered and smooth TiO_2 NTs, see Fig. 1(c-3)) and also significantly enhance the application performances of the obtained NTs (see Fig. 4).

4. Conclusion

In summary, the TiO_2 NTs are prepared on three different Ti substrates in the unique HBF_4-based electrolyte. It is shown that the formed TiO_2 NTs have hierarchical upper-porous and lower-tubular structure, and as revealed by the XPS results, the F 1s and B 1s elements are successfully doped into the TiO_2 NTs. The influence of Ti substrates on the surface morphology and properties of the obtained TiO_2 NTs is investigated. The TiO_2 NTs grown on the rough abraded Ti have very small inner tube diameter and weak ordered structure, hence show poor PEC performance. The formed TiO_2 NTs on the elelctropolished Ti substrate are relatively ordered, while have very rough sidewalls. The TiO_2 NTs produced by two-step anodization show the best PEC performance among the three samples due to their highly ordered structure and very smooth tube walls. The Ti substrate morphology has great influence on the growth of TiO_2 NTs, especially in the initial tube formation stage.

Acknowledgements

The authors would like acknowledge the financial support from the National Natural Science Foundation of China (NSFC, NO. 20976058).

References

[1] V. Zwilling, D. David, M.Y. Perrin, M. Aucouturier, Surf. Interface Anal. 637 (1999) 629.
[2] D. Gong, C. Grimes, O.K. Varghese, W. Hu, R. Singh, Z. Chen, E.C. Dickey, J. Mater. Res. 16 (2001) 3331.
[3] P. Roy, S. Berger, P. Schmuki, Angew. Chem. Int. Ed. 50 (2011) 2904.
[4] I. Paramasivam, H. Jha, N. Liu, P. Schmuki, Small 8 (2012) 3073.
[5] J.M. Macak, H. Tsuchiya, L. Taveira, S. Aldabergerova, P. Schmuki, Angew. Chem. Int. Ed. 44 (2005) 7463.
[6] H.E. Prakasam, K. Shankar, M. Paulose, O.K. Varghese, C.A. Grimes, J. Phys. Chem. C 111 (2007) 7235.
[7] Z. Su, W. Zhou, Adv. Mater. 20 (2008) 3663.
[8] A. Valota, D. LeClere, P. Skeldon, M. Curioni, T. Hashimoto, S. Berger, J. Kunze, P. Schmuki, G. Thompson, Electrochim. Acta 54 (2009) 4321.
[9] D. Kim, A. Ghicov, S.P. Albu, P. Schmuki, J. Am. Chem. Soc. 130 (2008) 16454.
[10] I. Paramasivam, J.M. Macak, T. Selvam, P. Schmuki, Electrochim. Acta 54 (2008) 643.
[11] S.E. John, S.K. Mohapatra, M. Misra, Langmuir 25 (2009) 8240.
[12] H. Wender, A.F. Feil, L.B. Diaz, C.S. Ribeiro, G.J. Machado, P. Migowski, D.E. Weibel, J. Dupont, S.R. Teixeira, Acs Appl. Mater. Interfaces 3 (2011) 1359.
[13] H. Li, J. Qu, Q. Cui, H. Xu, H. Luo, M. Chi, R.A. Meisner, W. Wang, S. Dai, J. Mater. Chem. 21 (2011) 9487.
[14] H. Li, S.K. Martha, R.R. Unocic, H. Luo, S. Dai, J. Qu, J. Power Sources 218 (2012) 88.
[15] Y. Yang, S.P. Albu, D. Kim, P. Schmuki, Angew. Chem. 123 (2011) 9237.
[16] K. Zhu, T.B. Vinzant, N.R. Neale, A.J. Frank, Nano Lett. 7 (2007) 3739.
[17] A. Seyeux, S. Berger, D. LeClere, A. Valota, P. Skeldon, G.E. Thompson, J. Kunze, P. Schmuki, J. Electrochem. Soc. 156 (2009) K17.

[18] J.H. Xing, Z.B. Xia, J.F. Hu, Y.H. Zhang, L. Zhong, J. Electrochem. Soc. 160 (2013) C239.
[19] D. Kim, A. Ghicov, P. Schmuki, Electrochem. Commun. 10 (2008) 1835.
[20] Y.R. Smith, B. Sarma, S.K. Mohanty, M. Misra, Int. J. Hydrogen. Energ (2013) 2062.
[21] Y. Shin, S. Lee, Nano Lett. 8 (2008) 3171.
[22] S. Li, G. Zhang, D. Guo, L. Yu, W. Zhang, J. Phys. Chem. C 113 (2009) 12759.
[23] H. Masuda, K. Fukuda, Science 268 (1995) 1466.
[24] H. Masuda, H. Yamada, M. Satoh, H. Asoh, M. Nakao, T. Tamamura, Appl. Phys. Lett. 71 (1997) 2770.
[25] Z. Zhang, Y. Yu, P. Wang, Acs Appl. Mater. Interfaces 4 (2012) 990.
[26] F.X. Xiao, Acs Appl. Mater. Interfaces 4 (2012) 7055.
[27] Z. Zhang, P. Wang, Energy Environ. Sci. 5 (2012) 6506.
[28] J. Li, C.J. Lin, C.G. Lin, J. Electrochem. Soc. 158 (2011) C55.
[29] F. Wang, Y. Liu, W. Dong, M. Shen, Z. Kang, J. Phys. Chem. C 115 (2011) 14635.
[30] J. Xing, Z. Xia, J. Hu, Y. Zhang, L. Zhong, Corros. Sci. 75 (2013) 212.
[31] Z. Xia, H. Nanjo, H. Tetsuka, T. Ebina, M. Izumisawa, M. Fujimura, J. Onagawa, Electrochem. Commun. 9 (2007) 850.
[32] S. So, K. Lee, P. Schmuki, J. Am. Chem. Soc. 134 (2012) 11316.
[33] N. Lu, X. Quan, J. Li, S. Chen, H. Yu, G. Chen, J. Phys. Chem. C 111 (2007) 11836.
[34] Y. Yu, H.H. Wu, B.L. Zhu, S.R. Wang, W.P. Huang, S.H. Wu, S.M. Zhang, Catal. Lett. 121 (2008) 165.
[35] J. Li, N. Lu, X. Quan, S. Chen, H. Zhao, Ind. Eng. Chem. Res. 47 (2008) 3804.
[36] Z. Zhang, M.F. Hossain, T. Takahashi, Int. J. Hydrogen. Energ 35 (2010) 8528.
[37] M. Ye, X. Xin, C. Lin, Z. Lin, Nano Lett. 11 (2011) 3214.
[38] L. Taveira, J. Macak, H. Tsuchiya, L. Dick, P. Schmuki, J. Electrochem. Soc. 152 (2005) B405.
[39] K. Yasuda, J.M. Macak, S. Berger, A. Ghicov, P. Schmuki, J. Electrochem. Soc. 154 (2007) C472.
[40] J.M. Macak, H. Tsuchiya, P. Schmuki, Angew. Chem. Int. Ed. 44 (2005) 2100.
[41] L. Xiao, K.E. Johnson, J. Electrochem. Soc. 150 (2003) E307.
[42] J.H. Xing, H. Li, Z.B. Xia, J.F. Hu, Y.H. Zhang, L. Zhong, J. Electrochem. Soc. 160 (2013) C503.